中国光学（中英文） Chinese Optics 核心期刊

Enhanced performance in AlGaN deep-ultraviolet laser diodes without an electron blocking layer by using a thin undoped $Al_{0.8}Ga_{0.2}N$ strip layer structure

SANG Xi-en, WANG Fang, LIU Jun-jie, LIU Yu-huai

Citation:
SANG Xi-en, WANG Fang, LIU Jun-jie, LIU Yu-huai. Enhanced performance in AlGaN deep−ultraviolet laser diodes without an electron blocking layer by using a thin undoped $Al_{0.8}Ga_{0.2}N$ strip layer structure[J]. *Chinese Optics*, In press. doi: 10.37188/CO.EN−2025−0033
桑恩, 王芳, 刘俊杰, 刘玉怀. 通过使用无掺杂的$Al_{0.8}Ga_{0.2}N$条状薄层结构提高无电子阻挡层的AlGaN深紫外激光二极管的性能[J]. 中国光学, 优先发表. doi: 10.37188/CO.EN−2025−0033

View online: https://doi.org/10.37188/CO.EN−2025−0033

Articles you may be interested in

Continuous deep ultraviolet laser by intracavity frequency doubling of blue laser diode pumped Pr：YLF
蓝光二极管抽运Pr：YLF腔内倍频连续深紫外激光器
Chinese Optics. 2021, 14(6): 1395 https://doi.org/10.37188/CO.2021−0077

High repetition frequency 257 nm deep ultraviolet picosecond laser with 5.2 W output power
5.2 W高重频257 nm深紫外皮秒激光器
Chinese Optics. 2023, 16(6): 1318 https://doi.org/10.37188/CO.2023−0026

Blue−blocking optical thin films with controllable cutoff slope
截止斜率可控的蓝光防护光学薄膜
Chinese Optics. 2021, 14(3): 544 https://doi.org/10.37188/CO.2020−0212

Strategies for improving the stability of quantum dots light−emitting diodes
量子点发光二极管稳定性提高策略
Chinese Optics. 2021, 14(1): 117 https://doi.org/10.37188/CO.2020−0184

Film thickness uniformity of deep ultraviolet large aperture aspheric mirror
深紫外大口径非球面反射膜的均匀性研究
Chinese Optics. 2022, 15(4): 740 https://doi.org/10.37188/CO.2022−0005

Fabrication and characterization of an LED based on a GaN−on−silicon platform with an ultra−thin freestanding membrane in the blue range
电致发光的完全悬空超薄硅衬底氮化镓基蓝光LED器件的制备与表征
Chinese Optics. 2021, 14(1): 153 https://doi.org/10.37188/CO.2020−0148

文章编号　2097-1842(xxxx)x-0001-13

Enhanced performance in AlGaN deep-ultraviolet laser diodes without an electron blocking layer by using a thin undoped $Al_{0.8}Ga_{0.2}N$ strip layer structure

SANG Xi-en[1], WANG Fang[1,2,3,4*], LIU Jun-jie[5], LIU Yu-huai[1,2,3,4*]

(1. *National Center for International Joint Research of Electronic Materials and Systems*, *International Joint-Laboratory of Electronic Materials and Systems of Henan Province*, *School of Electrical and Information Engineering*, *Zhengzhou University*, *Zhengzhou*, *Henan* 450001, *P. R. China*;

2. *Institute of Intelligence Sensing*, *Zhengzhou University*, *Zhengzhou*, *Henan* 450001, *P. R. China*;

3. *Research Institute of Industrial Technology Co. Ltd.*, *Zhengzhou University*, *Zhengzhou*, *Henan* 450001, *P. R. China*;

4. *Zhengzhou Way Do Electronics Co. Ltd.*, *Zhengzhou*, *Henan* 450001, *P. R. China*;

5. *School of Electrical and Information Engineering*, *North Minzu University*, *Yinchuan*, *Ningxia* 750001, *P. R. China*)

* *Corresponding author*, *E-mail*: *iefwang@zzu.edu.cn*; *ieyhliu@zzu.edu.cn*

Abstract: AlGaN-based deep-ultraviolet (DUV) laser diodes (LDs) face performance challenges due to electron leakage and poor hole injection, often worsened by polarization effects from conventional electron blocking layers (EBLs). To overcome these limitations, we propose an EBL-free DUV LD design incorporating a 1-nm undoped $Al_{0.8}Ga_{0.2}N$ thin strip layer after the last quantum barrier. Using PICS3D simulations, we evaluate the optical and electrical characteristics. Results show a significant increase in effective electron barrier height (from 158.2 meV to 420.7 meV) and a reduction in hole barrier height (from 149.2 meV to 62.8 meV), which enhance carrier injection and reduce leakage. The optimized structure (LD3) achieves a 14% increase in output power, improved slope efficiency (1.85 W/A), and lower threshold current. This design also reduces the quantum confined Stark effect and forms dual hole accumulation regions, improving recombination efficiency. Our findings present a promising approach for high-performance, EBL-free DUV LDs suitable for high-power applications.

Key words: AlGaN; deep ultraviolet laser diodes; undoped thin strip structure; without an electron blocking layers

收稿日期：2025-06-16；**修订日期**：xxxx-xx-xx

基金项目：国家自然科学基金（No. 62174148）；国家重点研发计划（No. 2022YFE0112000）；河南省国际科技合作重点项目（No. 231111520300）

Supported by National Nature Science Foundation of China (No. 62174148); National Key Research and Development Program (NKRDP Grant No. 2022YFE0112000); Key Program for International Joint Research of Henan Province (No. 231111520300).

通过使用无掺杂的 $Al_{0.8}Ga_{0.2}N$ 条状薄层结构提高无电子阻挡层的 AlGaN 深紫外激光二极管的性能

桑習恩[1], 王　芳[1,2,3,4*], 刘俊杰[5], 刘玉怀[1,2,3,4*]
（1. 郑州大学电气与信息工程学院, 电子材料与系统国际联合研究中心, 河南省电子材料与系统国际联合实验室, 郑州 450001;
2. 教育部集成电路设计与应用国际合作联合实验室, 郑州 450001;
3. 郑州大学智能传感研究院, 郑州大学产业技术研究院有限公司, 郑州 450001;
4. 郑州唯独电子科技有限公司, 郑州 450001;
5. 北方民族大学电气与信息工程学院, 银川 750001）

摘要: 基于氮化铝的深紫外激光二极管通常使用电子阻挡层来防止电子泄漏到 p 型区。然而, 电子阻挡层也会阻碍空穴注入有源区, 导致激光效率降低。为了解决这个问题, 我们建议在最后一个量子势垒之后使用未掺杂的薄 $Al_{0.8}Ga_{0.2}N$ 条状结构来代替电子阻挡层。研究结果表明, 与使用 电子阻挡层 的传统激光设计相比, 1 nm $Al_{0.8}Ga_{0.2}N$ 带状层可以通过增加有效势垒高度来有效抑制电子泄漏并增强空穴注入。有源区的载流子浓度和量子阱的重组效率提高, 进而增加了激光器的输出功率。

关　键　词: AlGaN; 深紫外激光器; 未掺杂条状薄层; 无电子阻挡层
中图分类号: O472　　**文献标志码:** A　　**doi:** 10.37188/CO.EN-2025-0033　　**CSTR:** 32171.14.CO.EN-2025-0033

1 Introduction

The current deep ultraviolet (DUV) laser diode (LD) exhibits significant potential for a range of applications, including transportation, bio-detection, medical phototherapy, and water purification[1-5]. Compared to conventional mercury lamps, DUV LDs offer advantages such as extended lifespan, enhanced energy efficiency, and environmental sustainability[6-8]. Consequently, these devices have garnered increasing attention from researchers over recent decades. However, a notable challenge remains: a substantial decline in device performance with increasing current, which continues to hinder their application in high-power contexts[9-10]. Several factors have been identified as contributing to this efficiency degradation, including electron leakage[11-12], low hole injection efficiency[13], high carrier dislocation density[14], and Auger recombination[15-17], The higher mobility of electrons relative to holes results in electron spillover and significant energy loss[18-19]. To address these issues, a variety of solutions have been proposed. For instance, the use of dilute-As GaNAs has been suggested to reduce interband Auger recombination[20]. Zhang et al. achieved a lower threshold current by reducing the threshold gain by improving the optical confinement factor and epitaxial growth conditions in the 274.8 nm emission wavelength band. In addition, the laser operating voltage was reduced by using a double-sided n-electrode arrangement[21]. Zhang et al. systematically changed the quantum well width and found that the 3 nm narrow quantum well had a higher material gain coefficient and a lower transparent carrier density, thereby achieving a lower threshold current density, indicating that it is more suitable for achieving high-efficiency laser output[22]. Additionally, to mitigate electron leakage and enhance carrier injection, approaches such as the substitution of AlGaN with BGaN material for electron leakage prevention[23], Zhang et al. designed the symmetrical step-shaped electron and hole blocking layers (HBL)[24]. However, introducing an EBL with

a high aluminum component can only alleviate the electron leakage problem to a certain extent. The ionization energy of Mg-doped AlGaN layers is enhanced with the increase of Al content. Achieving high p-type conductivity in a high Al content AlGaN layer is difficult. As a result, the hole concentration in the p-region is limited[25]. Furthermore, polarized charge regions can form at the interface between the EBL and the QW, leading to electron accumulation near the last QW of the p-type layer, thereby exacerbating electron leakage. Additionally, the lattice mismatch between the final potential barrier layer and the EBL induces strong polarization effects, resulting in severe energy band bending in the EBL[26], This bending reduces the effective electron barrier height while increasing the effective hole barrier height, making hole injection into the active region more difficult. To address these issues, several researchers have proposed EBL-free structures. For example, Zhang et al. eliminated the EBL by utilizing p-type doped barriers and low Al mole fraction HBLs to improve light-emitting diode (LED) performance[27], Zhang et al. used a distributed polarization-doped p-cladding layer on a model without an electron blocking layer to achieve lower internal losses and high hole injection rates in the device[28], Sharif et al. proposed the structure of graded hole source layer without EBL to improve the performance of deep-ultraviolet nanowire LED[29], Velpula et al. proposed improving carrier transport in AlGaN deep-ultraviolet LED using a strip-in-a-barrier structure[30]. However, most studies focusing on EBL removal are centered on LED applications, with few addressing LDs. In this work, We propose a structure that eliminates the electron blocking layer (EBL) under the condition of a 267 nm emission wavelength. By removing the traditional EBL layer, this structure effectively reduces the band bending caused by polarization effects. Furthermore, the introduction of an undoped thin strip layer reduces the quantum confined Stark effect (QCSE) in the active region[31], increases the electron barrier height, and prevents electron leakage from the active region to the p-type region, thereby improving the stability and efficiency of the laser, particularly in high-power applications. Experimental comparative analysis shows that this structure also lowers the hole barrier height, facilitating hole injection, which effectively enhances carrier injection and recombination efficiency, thus improving the laser performance and mitigating efficiency degradation. Finally, we optimized the thickness of the thin layers (1 nm, 2 nm, 3 nm, 4 nm) and the Al composition (0.6, 0.65, 0.7, 0.75, 0.8). Our findings indicate that a 1 nm $Al_{0.8}Ga_{0.2}N$ thin layer structure optimally enhances device performance, playing an important role in advancing high-power deep ultraviolet laser applications.

2 Simulation structure and parameters

Figure 1(a) is a schematic diagram of a DUV LD using sapphire as the substrate. The laser structure consists of a 0.1-μm-thick $Al_{0.75}Ga_{0.25}N$ $Al_{0.75}Ga_{0.25}N$ contact layer, a 1-μm-thick $Al_{0.75}Ga_{0.25}N$ $Al_{0.75}Ga_{0.25}N$ cladding (n-CL), a 0.11-μm-thick $Al_{0.68}Ga_{0.32}N$ $Al_{0.68}Ga_{0.32}N$ lower waveguide layer (LWG), multiple quantum wells (MQWs) composed of two 3-nm thick $Al_{0.58}Ga_{0.42}N$ $Al_{0.58}Ga_{0.42}N$ wells (QWs) and three 8-nm-thick $Al_{0.68}Ga_{0.32}N$ $Al_{0.68}Ga_{0.32}N$ barriers (QBs), The P-type region includes a 20-nm-thick $Al_{0.7}Ga_{0.3}N$ $Al_{0.7}Ga_{0.3}N$ EBL, a 0.7-μm-thick $Al_{0.68}Ga_{0.32}N$ $Al_{0.68}Ga_{0.32}N$ upper waveguide (UWG), a 0.4-μm-thick $Al_{0.75}Ga_{0.25}N$ $Al_{0.75}Ga_{0.25}N$cladding (p-CL) and a 0.1-μm-thick $Al_{0.8}Ga_{0.2}NAl_{0.8}Ga_{0.2}N$ contact layer. Insert a 1 nm thick $Al_{0.8}Ga_{0.2}N$ $Al_{0.8}Ga_{0.2}N$ undoped thin layer between the LQB and the EBL for LD2 structure. The LD3 structure is based on the LD2 structure with the EBL removed. The structure diagram of LD1, LD2, and LD3 is shown in Figure 1(b). Analyze the optical and electrical properties of devices with the Advanced Physical Model

for Semiconductor Devices (PICS3D) developed by Crosslight Software Inc[32]. PICS3D software calculates the electrical behavior of all LDs by solving Poisson's equation and the current continuity equation for electrons and holes[33]. In this simulation, the p- and n-electrodes were considered ideal ohmic contacts. According to the experimental conditions, the ambient temperature is set to 300 K, the laser cavity length is 530 μm, the width is 3 μm, the return loss is 2400, and the specular refractive index is 30%[34]. Spontaneous polarization and piezoelectric polarization were carefully designed with the method proposed by Fiorentini et al.[35]. The LD structure is a Fabry– Perot cavity modified from the GaN blue LD proposed by Nakamura and Fasol[36]. Other detailed material parameters can be found in the reference[37].

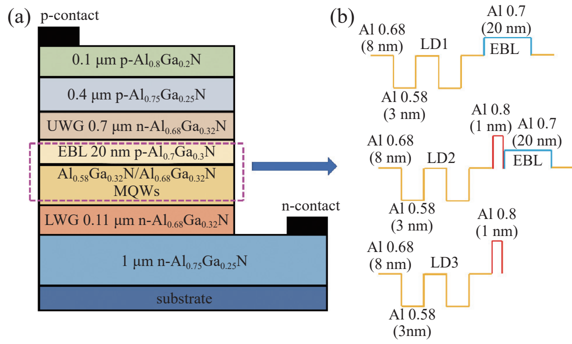

Fig. 1 (a) Schematics of the DUV-LD structure, and (b) LD1, LD2, and LD3 structure diagram

3 Results and Discussion

To elucidate the physical mechanisms underpinning the improved performance of the proposed structure, we analyze the effect of the undoped $Al_{0.8}Ga_{0.2}N$ thin strip layer on band structure modulation. The introduction of this high-Al-content layer at the interface induces a polarization field redistribution, which partially compensates for the spontaneous and piezoelectric polarization discontinuities between adjacent AlGaN layers. This compensation reduces the magnitude of built-in electric fields and thereby alleviates the severe band bending commonly observed in conventional DUV-LD heterostructures.

The suppression of band bending enhances carrier confinement by reshaping the conduction and valence band profiles. In particular, the reduced downward bending of the conduction band increases the effective electron barrier height, while the smoothed valence band profile reduces the hole injection barrier. Moreover, due to the disparity in effective masses between electrons and holes in high-Al-content AlGaN materials, the quasi-Fermi level separation plays a critical role in modulating carrier accumulation. The high effective mass of holes leads to a broader spatial distribution under a given Fermi level shift, facilitating better overlap with the quantum well region.

Additionally, the thin and undoped nature of the inserted $Al_{0.8}Ga_{0.2}N$ layer minimizes ionized impurity scattering, preserving mobility and enabling efficient tunneling-assisted injection. The resulting structure promotes balanced carrier injection and recombination, which is essential for improving efficiency and threshold current characteristics in DUV laser diodes.

To study the performance of the proposed structure, we conducted a numerical analysis to investigate the three LDs. First, we calculated the energy band diagrams of the LD1, LD2, and LD3. The principle of improving hole injection and electron leakage is to reduce the effective barrier height of the valence band and increase the effective barrier height of the conduction band[38]. The effective barrier height is defined as the energy difference between an energy band and its corresponding quasi-Fermi level[39]. It is a reliable parameter for evaluating a laser's electron confinement ability and hole injection efficiency.

As illustrated in Figure 2, the electron effective barrier height for LD1 is 158.2 meV, which is relatively low compared to LD2, where an undoped strip thin layer has been incorporated. After eliminating the EBL, the effective potential barrier for LD3 rises to 420.7 meV, significantly hindering

electron leakage. In contrast, the effective potential barrier for holes in LD3 is 62.8 meV, which is lower than that of LD1 (149.2 meV) and LD2 (261.2 meV), thereby minimizing the resistance to hole injection into the active region. This reduction in hole injection barrier primarily arises due to the polarization charge generated at the heterointerface between the LQB and the EBL, which causes a sharp band bending in the conduction band, thereby lowering the effective barrier height for electrons while simultaneously increasing the barrier for holes. Furthermore, this polarization effect results in the accumulation of electrons in this region, contributing to the formation of nonradiative recombination centers[40] thereby exacerbating electron leakage.

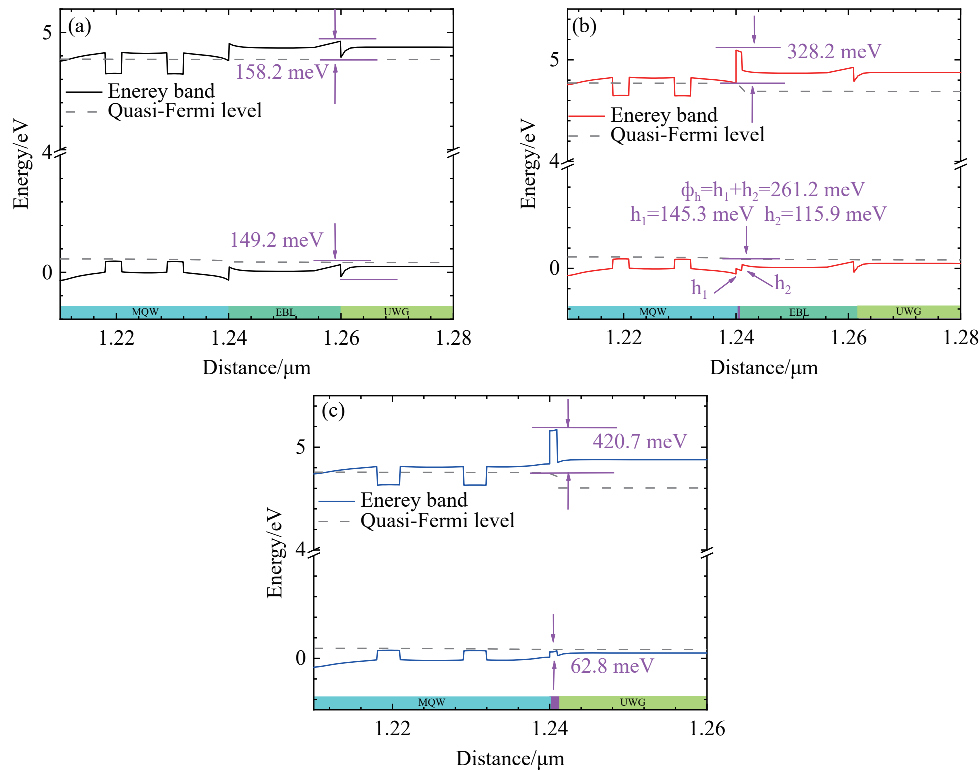

Fig. 2　Energy band diagram and quasi-fermi level (a) LD1, (b) LD2, and (c) LD3

Additionally, a hole depletion region forms at the LQB-EBL heterointerface due to the polarization effect, as shown in Figure 2(a), which further limits hole injection efficiency. However, the insertion of the thin strip layer mitigates the impact of this depletion region, creating a hole accumulation zone, as seen in Figure 2(b). In the absence of the EBL structure, LD3 eliminates the hole depletion region entirely, forming two distinct hole accumulation regions, as depicted in Figure 2(c), which further enhances hole injection efficiency.

To further validate the proposed structure, we examine the electron and hole concentrations in the three LD configurations, as shown in Figure 3. The removal of the EBL in LD3 eliminates the energy band bending caused by the polarization charge, which in turn elevates the pulled-down energy band. This leads to an increase in the effective electron barrier height, thereby reducing electron leakage into the p-type region. As illustrated in Figure 3(a), the electron concentration in the p-type region of LD3 is the lowest when compared to LD1 and LD2. Additionally, LD3 reduces the effective hole barrier height, facilitating hole injection into the active region. As shown in Figure 3(b), the highest hole concentration is observed in the thin strip layer of LD3, which further supports our previous analysis.

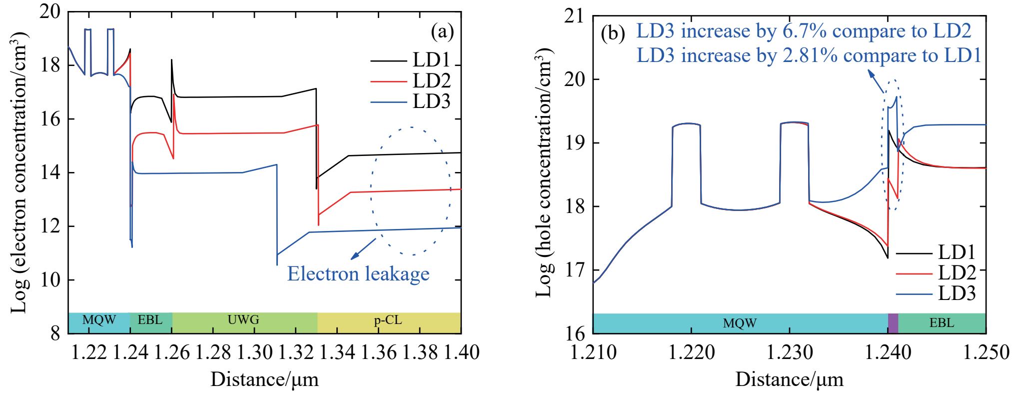

Fig. 3 (a) Electron leakage in the p-type region of three structures, and (b) hole concentration of the three structures

As a result, the output power of LD3 shows a significant improvement compared to LD1 and LD2. As demonstrated in Figures 4(a), and 4(b), the output power of LD3 increases to 100.2 mW, surpassing that of LD1 (87 mW) and LD2 (91 mW). Additionally, the slope efficiency of LD3 reaches 1.8 W/A, representing improvements of 12% and 8% over LD1 (1.6 W/A) and LD2 (1.7 W/A), respectively. Furthermore, the threshold current for LD3 is reduced to 24 mA, which is lower than that of LD1 (26 mA) and LD2 (25 mA), and the threshold voltage of LD3 is 4.623 V, which is also lower than that of LD1 (4.629 V) and LD2 (4.632 V). These improvements can be attributed to the higher carrier concentration in the active region of LD3, as shown in Figures 5(a), and 5(b).

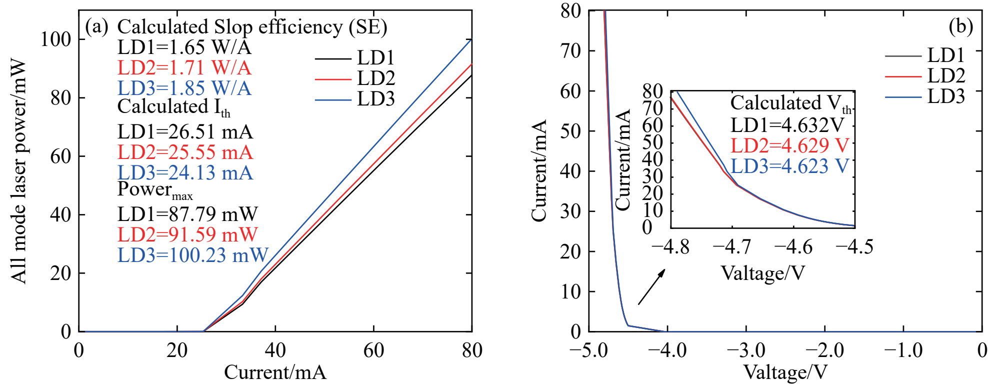

Fig. 4 (a) P-I curve of three structures, and (b) I-V curve of three structures

Although our simulations primarily focus on carrier transport, band structure modulation, and radiative recombination efficiency, these improvements have important implications for room-temperature (RT) lasing feasibility. A key prerequisite for RT lasing in DUV laser diodes is a low threshold current density, which is strongly influenced by the balance of carrier injection and recombination rates.

The proposed EBL-free structure with a strip layer ctructure enhances both hole injection and electron confinement, thereby improving the spatial overlap of electrons and holes in the quantum wells and increasing efficiency. These enhancements effectively reduce the carrier density required to reach population inversion, leading to a lower lasing threshold.

Furthermore, the improved optical power observed in LD 3 indicates reduced nonradiative losses and more efficient radiative recombination, which are essential for maintaining high optical gain at room temperature.

Additionally, in AlGaN-based materials, holes exhibit a relatively high effective mass and low mobility compared to electrons, leading to a non-uniform distribution of holes within the multiple quantum well (MQW) structure. Consequently, holes

near the p-side of the MQW accumulate at higher concentrations than those near the n-side[41-42], which enhances the effective radiative recombination rate within the MQW, as illustrated in Figure 5(c). This increased radiative recombination in the active region leads to a lower threshold current for LD3, as shown in Figure 5(d), further improving the optoelectronic properties of the device.

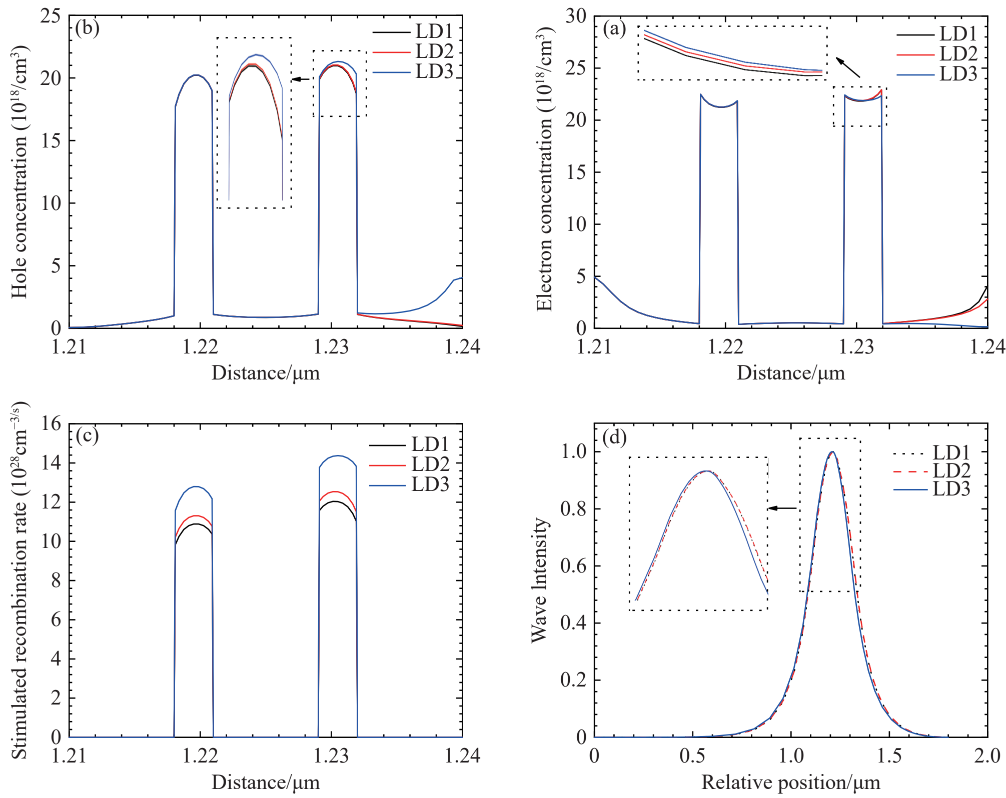

Fig. 5 (a) The electron concentration in the MQWs, (b) the hole concentration in the MQWs, (c) stimulated recombination rate in MQWs, and (d) numerically calculated near-field optical model profile for LD1, LD2, and LD3

To gain deeper insight into the device performance, we calculated the electron and hole current densities for LD1, LD2, and LD3. As shown in Figure 6(a), the increased effective electron potential barrier height in LD3 significantly reduces electron leakage. In Figure 6(b), LD3, by removing the energy band bending caused by the polarization charge effect at the EBL-LQB interface, forms a hole accumulation region. This not only improves hole injection but also reduces the energy loss of holes during transport, leading to enhanced device performance.

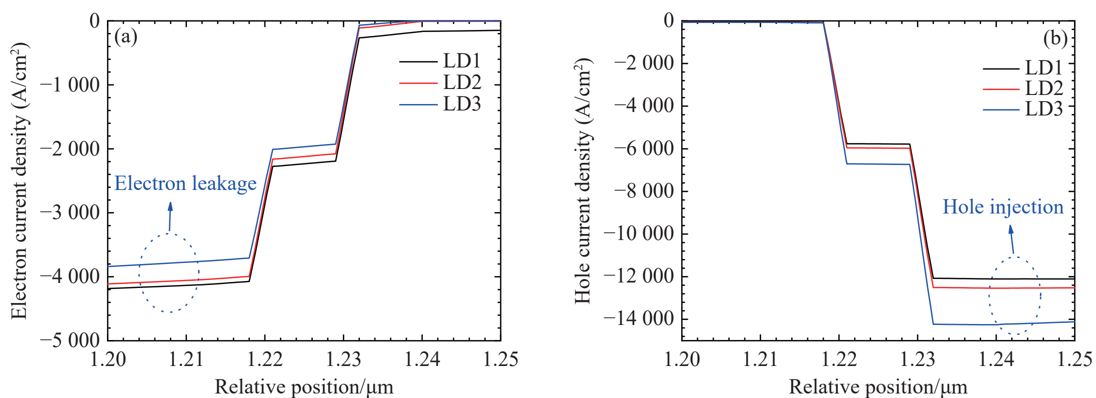

Fig. 6 (a) Electron current density of three structures, and (b) hole current density of three structures

We further investigated the performance of LD2 with an inserted undoped thin strip structure of $Al_xGa_{1-x}N$, varying the Al component and thickness. As shown in Figures 7(a), and 7(b), the output power and radiative recombination rate of LD2 are maximized when the Al component is 0.8, yielding the best laser performance. This improvement is attributed to the insertion of the undoped thin strip structure between the EBL and the LQB of LD2, which effectively mitigates the band bending caused by polarization at the heterogeneous interfaces, thereby enhancing device performance. At lower Al components, however, the electron confinement in the QW weakens, leading to increased electron leakage into the p-region, which negatively impacts the radiative recombination rate. When the Al component is 0.8, the electron effective potential barrier is at its highest, leading to stronger electron confinement in the MQW. Furthermore, the formation of a hole accumulation region at the heterogeneous interface reduces the hole depletion region, thereby improving hole injection efficiency, increasing carrier concentration in the active region, and consequently enhancing the effective recombination rate and output power.

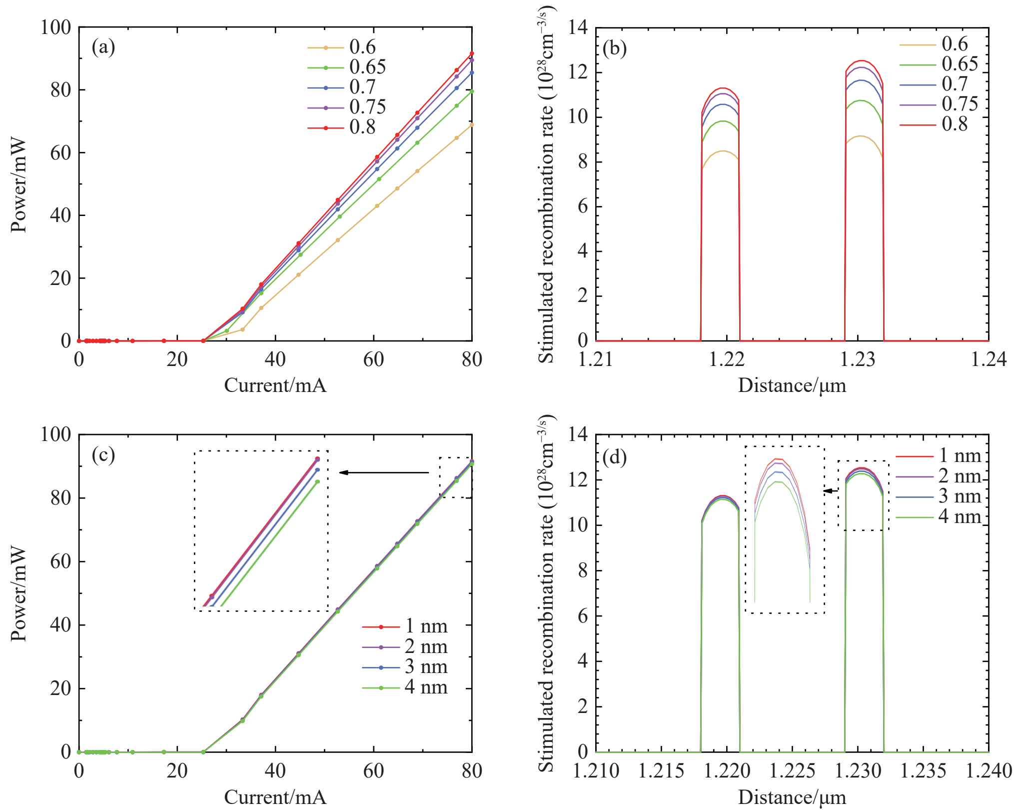

Fig. 7 (a) LD2 output power of different Al components, (b) LD2 recombination rates of different Al components in MQWs, (c) output power with different thickness of $Al_{0.8}Ga_{0.2}N$ strip of LD2, and (d) recombination rates with different thickness of $Al_{0.8}Ga_{0.2}N$ $Al_{0.8}Ga_{0.2}N$strip of LD2 in MQWs

Figures 7(c), and 7(d) reveal that the device performance is optimized when the thickness of the $Al_{0.8}Ga_{0.2}N$ thin strip structure is 1 nm. As the strip thickness increases, the ability of the cavities to enter the active region diminishes, reducing carrier injection efficiency and thereby lowering the effective recombination rate and output power. Therefore, the insertion of a 1 nm $Al_{0.8}Ga_{0.2}N$ thin strip layer effectively reduces the impact of strong polarization effects, optimizing device performance.

Building on these findings, we applied the conclusion to the removal of the EBL structure in LD3. As shown in Figure 8, the insertion of a 1 nm $Al_{0.8}Ga_{0.2}N$ thin strip layer in LD3 further enhances

device performance. This improvement is primarily due to the absence of the EBL layer in LD3, which prevents the strong polarization effects that typically lead to band bending. The thin strip layer increases the effective conduction band barrier height, better suppressing electron leakage, while simultaneously enhancing hole injection by inducing two hole accumulation regions at the thin layer. This significantly improves hole injection efficiency and overall device performance.

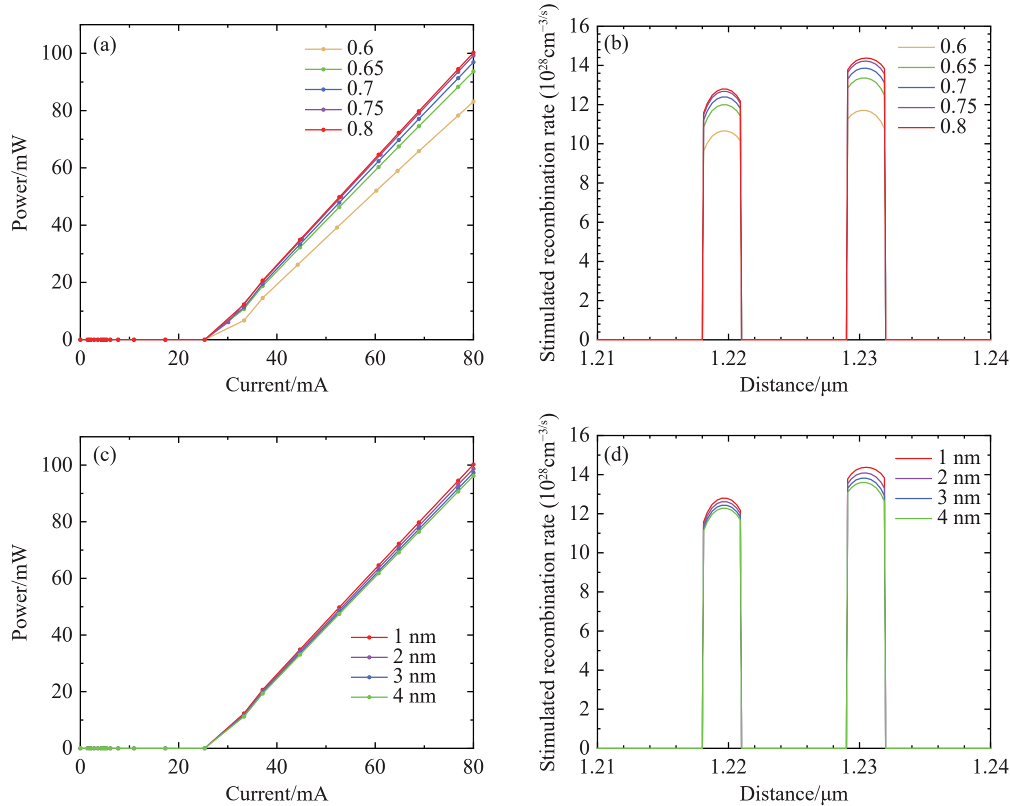

Fig. 8　(a) LD3 output power of different Al components, (b) LD3 recombination rates of different Al components in MQWs, (c) output power with different thickness of $Al_{0.8}Ga_{0.2}N$ $Al_{0.8}Ga_{0.2}N$strip of LD3, and (d) recombination rates with different thickness of $Al_{0.8}Ga_{0.2}N$ strip of LD3 in MQWs

Finally, Figure 9 illustrates the electric field distribution at the heterojunction. In Figure 9(a), it is evident that the electric field at the heterojunction surface varies with different Al compositions, with the minimal electric field occurring at an Al composition of 0.8. Figure 9(b) further analyzes the effect of thin layer thickness on the electric field when the Al composition is fixed at 0.8. It shows that the electric field at the heterojunction surface is minimal when the strip thickness is 1 nm. The electric field is closely related to the piezoelectric polarization charge density, and the small electric field at the heterogeneous interface reduces the polarization effect, thereby minimizing band bending, preventing electron leakage, and enhancing hole injection efficiency.

To evaluate the practical applicability of the proposed EBL-free structure, we qualitatively analyze its potential for supporting electrically injected lasing under realistic fabrication conditions. Several critical parameters—including modal gain, optical confinement factor, and threshold current density—must be considered when transitioning from simulation models to actual device processing.

First, the improved carrier injection balance in LD3 enhances radiative recombination within the multiple quantum wells (MQWs), directly contributing to higher modal gain. This is further supported

by the increased carrier concentration and stimulated recombination rate observed in our simulation. Moreover, the reduction of non-radiative centers at the heterointerfaces, due to the elimination of the EBL and the suppression of polarization-induced band bending, suggests that optical losses associated with carrier leakage can be minimized—favorably influencing threshold conditions.

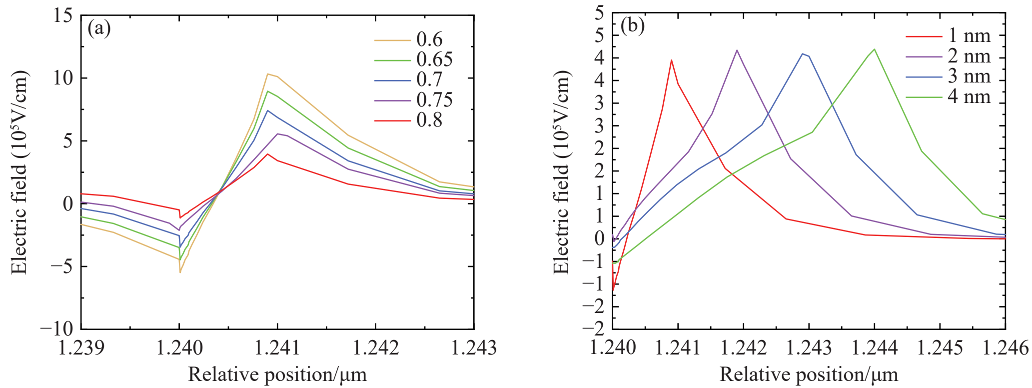

Fig. 9 (a) Electric field distribution of different al components of LD3, (b) Electric field distribution of LD3 with different thicknes

Second, the thin undoped $Al_{0.8}Ga_{0.2}N$ strip layer contributes to a more symmetric band profile and facilitates better waveguide index matching. This structural refinement can improve the optical confinement factor without the detrimental refractive index discontinuities often introduced by high-Al-content EBLs. Better confinement leads to more efficient overlap between the optical mode and the gain region, further enhancing the prospects for lasing.

Additionally, lateral current spreading in high-resistance p-type layers remains a well-known limitation in AlGaN-based DUV LDs. The removal of the EBL can reduce the overall series resistance of the p-type region, slightly improving lateral current uniformity. However, proper p-type contact engineering remains essential. To address this, strategies such as employing transparent current-spreading layers or highly doped graded-contact structures may be necessary to ensure uniform carrier injection across the ridge width.

Optical loss associated with the p-type cladding and contact layers is another practical concern. In our proposed structure, the Al content of the p-type waveguide and cladding is carefully chosen to reduce absorption while maintaining index contrast for confinement. Additionally, future designs may benefit from inserting electron-blocking-free hole injection layers that are both optically transparent and electrically conductive.

In summary, although this study primarily focuses on simulation-based optimization, the structural features introduced here—particularly the elimination of EBL-induced polarization effects and the tailored insertion of the undoped thin strip layer—provide a foundation for designing practical, electrically injected DUV LDs. With proper cavity design, thermal management, and current spreading optimization, the proposed structure holds strong potential for achieving low-threshold lasing at or near room temperature

4 Conclusion

In this work, we proposed and analyzed a novel EBL-free AlGaN-based deep-ultraviolet laser diode structure utilizing a 1-nm undoped $Al_{0.8}Ga_{0.2}N$ thin strip layer inserted after the last quantum barrier. Through comprehensive numerical simulations, we demonstrated significant improvements in electron confinement, hole injection efficiency, carrier concentration in the active region, and overall radi-

ative recombination rate. The optimized structure (LD3) achieved a 14% increase in output power, reduced threshold current, and enhanced slope efficiency. These advancements stem from the suppression of polarization-induced band bending and the elimination of the hole depletion region typically introduced by conventional EBLs.

Importantly, this work offers a physically guided structural design framework that may enable low-threshold lasing at or near room temperature. Although room-temperature lasing is not directly demonstrated, the observed improvements strongly suggest that, with proper implementation of standard cavity and thermal management strategies, the proposed EBL-free structure has significant potential for experimental realization in high-performance DUV LD applications.

References:

[1] MURAMOTO Y, KIMURA M, NOUDA S. Development and future of ultraviolet light-emitting diodes: UV-LED will replace the UV lamp[J]. *Semiconductor Science and Technology*, 2014, 29(8): 084004.

[2] NAKAMURA S. Future technologies and applications of III-nitride materials and devices[J]. *Engineering*, 2015, 1(2): 161.

[3] KNEISSL M, SEONG T Y, HAN J, *et al*.. The emergence and prospects of deep-ultraviolet light-emitting diode technologies[J]. *Nature Photonics*, 2019, 13(4): 233-244.

[4] HINDS L M, O'DONNELL C P, AKHTER M, *et al*.. Principles and mechanisms of ultraviolet light emitting diode technology for food industry applications[J]. *Innovative Food Science & Emerging Technologies*, 2019, 56: 102153.

[5] HIRAYAMA H, MAEDA N, FUJIKAWA S, *et al*.. Recent progress and future prospects of AlGaN-based high-efficiency deep-ultraviolet light-emitting diodes[J]. *Japanese Journal of Applied Physics*, 2014, 53(10): 100209.

[6] 李文明, 常小辉. UVLED 在预防控制净水器细菌污染方面应用探讨[J]. 家电科技, 2020(2)：32-35.
LI W M, CHANG X H. Application of UVLED in prevention and control of bacterial pollution in water purifier[J]. *Journal of Appliance Science & Technology*, 2020(2): 32-35. (in Chinese).

[7] YU H B, REN ZH J, MEMON M H, *et al*.. Cascaded deep ultraviolet light-emitting diode via tunnel junction[J]. *Chinese Optics Letters*, 2021, 19(8): 082503.

[8] HIRAYAMA H. Research status and prospects of deep ultraviolet devices[J]. *Journal of Semiconductors*, 2019, 40(12): 120301.

[9] SATO K, YASUE S, YAMADA K, *et al*.. Room-temperature operation of AlGaN ultraviolet-B laser diode at 298 nm on lattice-relaxed $Al_{0.6}Ga_{0.4}N$/AlN/sapphire[J]. *Applied Physics Express*, 2020, 13(3): 031004.

[10] MUROTANI H, TANABE R, HISANAGA K, *et al*.. High internal quantum efficiency and optically pumped stimulated emission in AlGaN-based UV-C multiple quantum wells[J]. *Applied Physics Letters*, 2020, 117(16): 162106.

[11] GU W, LU Y, LIN R Y, *et al*.. BAlN for III-nitride UV light-emitting diodes: undoped electron blocking layer[J]. *Journal of Physics D: Applied Physics*, 2021, 54(17): 175104.

[12] SHI L, DU P, TAO G Y, *et al*.. High efficiency electron-blocking-layer-free deep ultraviolet LEDs with graded Al-content AlGaN insertion layer[J]. *Superlattices and Microstructures*, 2021, 158: 107020.

[13] LIU M R, LIU CH. Enhanced carrier injection in AlGaN-based deep ultraviolet light-emitting diodes by polarization engineering at the LQB/p-EBL interface[J]. *IEEE Photonics Journal*, 2022, 14(3): 8228005.

[14] CHANG J Y, HUANG M F, CHEN F M, *et al*.. Effects of quantum barriers and electron-blocking layer in deep-ultraviolet light-emitting diodes[J]. *Journal of Physics D: Applied Physics*, 2018, 15(7): 075106.

[15] DELANEY K T, RINKE P, VAN DE WALLE C G. Auger recombination rates in nitrides from first principles[J]. *Applied Physics Letters*, 2009, 94(19): 191109.

[16] IVELAND J, MARTINELLI L, PERETTI J, *et al*.. Direct measurement of Auger electrons emitted from a semiconductor light-emitting diode under electrical injection: identification of the dominant mechanism for efficiency droop[J]. *Physical Review Letters*, 2013, 110(17): 177406.

[17] TAN C K, ZHANG J, LI X H, *et al*.. First-principle electronic properties of dilute-as GaNAs alloy for visible light emitters[J]. *Journal of Display Technology*, 2013, 9(4): 272-279.

[18] HAI X, RASHID R T, SADAF S M, *et al*.. Effect of low hole mobility on the efficiency droop of AlGaN nanowire deep ultraviolet light emitting diodes[J]. *Applied Physics Letters*, 2019, 114(10): 101104.

[19] ZHANG ZH D, SUN H Q, LI X, *et al*.. Performance enhancement of blue light-emitting diodes with an undoped AlGaN electron-blocking layer in the active region[J]. *Journal of Display Technology*, 2016, 12(6): 573-576.

[20] TAN C K, TANSU N. Auger recombination rates in dilute-As GaNAs semiconductor[J]. *AIP Advances*, 2015, 5(5): 057135.

[21] ZHANG Z Y, KUSHIMOTO M, YOSHIKAWA A, *et al*.. Continuous-wave lasing of AlGaN-based ultraviolet laser diode at 274.8 nm by current injection[J]. *Applied Physics Express*, 2022, 15(4): 041007.

[22] ZHANG Z Y, KUSHIMOTO M, YOSHIKAWA A, *et al*.. Experimental study of gain characteristics in relation to quantum-well width of deep-ultraviolet laser diodes[J]. *Applied Physics Letters*, 2024, 125(18): 183505.

[23] XING ZH Q, WANG F, WANG Y, *et al*.. Enhanced performance in deep-ultraviolet laser diodes with an undoped BGaN electron blocking layer[J]. *Optics Express*, 2022, 30(20): 36446-36455.

[24] ZHANG A X, REN B Y, WANG F, *et al*.. Study of AlGaN-based deep ultraviolet laser diodes using one-way step-shaped quantum barriers and symmetrical step-shaped electron and hole blocking layers[J]. *Optical Engineering*, 2022, 61(10): 106101.

[25] NAKARMI M L, KIM K H, KHIZAR M, *et al*.. Electrical and optical properties of Mg-doped $Al_{0.7}Ga_{0.3}$ N alloys[J]. *Applied Physics Letters*, 2005, 86(9): 092108.

[26] VELPULA R T, JAIN B, LENKA T R, *et al*.. Polarization-engineered p-Type electron-blocking-layer-free III-nitride deep-ultraviolet light-emitting diodes for enhanced carrier transport[J]. *Journal of Electronic Materials*, 2022, 51(2): 838-846.

[27] ZHANG Y Y, FAN G H, ZHANG T. Performance enhancement of blue light-emitting diodes without an electron-blocking layer by using p-Type doped barriers and a hole-blocking layer of low Al mole fraction[J]. *IEEE Journal of Quantum Electronics*, 2012, 48(2): 169-174.

[28] ZHANG Z Y, KUSHIMOTO M, SAKAI T, *et al*.. A 271.8 nm deep-ultraviolet laser diode for room temperature operation[J]. *Applied Physics Express*, 2019, 12(12): 124003.

[29] SHARIF M N, USMAN M, NIASS M I, *et al*.. Compositionally graded AlGaN hole source layer for deep-ultraviolet nanowire light-emitting diode without electron blocking layer[J]. *Nanotechnology*, 2021, 33(7): 075205.

[30] VELPULA R T, JAIN B, BUI H Q T, *et al*.. Improving carrier transport in AlGaN deep-ultraviolet light-emitting diodes using a strip-in-a-barrier structure[J]. *Applied Optics*, 2020, 59(17): 5276-5281.

[31] WEINOLD M P, KOLESNIKOV S, ANADÓN L D. Rapid technological progress in white light-emitting diodes and its source in innovation and technology spillovers[J]. *Nature Energy*, 2025, 10(5): 616-629.

[32] PICS3D. Crosslight Software Inc. , Burnaby, Canada[EB/OL]. https://3390-ca.all.biz/.**(查阅网上资料,未能确认本条文献修改是否正确,请确认)(查阅网上资料,未找到引用日期,请补充)**.

[33] LIN R H, GALAN S V, SUN H D, *et al*.. Tapering-induced enhancement of light extraction efficiency of nanowire deep ultraviolet LED by theoretical simulations[J]. *Photonics Research*, 2018, 6(5): 457-462.

[34] YEN S H, KUO Y K. Polarization-dependent optical characteristics of violet InGaN laser diodes[J]. *Journal of Applied Physics*, 2008, 103(10): 103115.

[35] FIORENTINI V, BERNARDINI F, AMBACHER O. Evidence for nonlinear macroscopic polarization in III–V nitride alloy heterostructures[J]. *Applied Physics Letters*, 2002, 80(7): 1204-1206.

[36] NAKAMURA S, FASOL G. *The Blue Laser Diode: GaN Based Light Emitters and Lasers*[M]. Berlin: Springer, 1997.

[37] VURGAFTMAN I, MEYER J R, RAM-MOHAN L R. Band parameters for III–V compound semiconductors and their alloys[J]. *Journal of Applied Physics*, 2001, 89(11): 5815-5875.

[38] LI H, ZHANG J Y, WEN W, *et al*.. Highly efficient light-emitting diodes via self-assembled InP quantum dots[J]. *Nature Communications*, 2025, 16(1): 4257.

[39] ZHENG Y ZH, LIN X, LI J ZH, *et al*.. In situ n-doped nanocrystalline electron-injection-layer for general-lighting quantum-dot LEDs[J]. *Nature Communication*, 2025, 16(1): 3362.

[40] ZHANG Z Q, GENG H S, LV ZH X, *et al*.. Manipulating precursors of group-III nitrides for high-Al-content p-AlGaN toward efficient deep ultraviolet light emitters[J]. *Applied Physics Letters*, 2024, 125(24): 241109.

[41] JIANG ZH A, ZHU Y H, XIA CH SH, *et al*.. Enhanced characteristics in AlGaN-based deep ultraviolet light-emitting

diodes with interval-graded barrier superlattice electron blocking layers[J]. *Micro and Nanostructures*, 2024, 191: 207869.

[42] ZHU X T, LUO X, DENG Y ZH, *et al*.. Doping bilayer hole-transport polymer strategy stabilizing solution-processed green quantum-dot light-emitting diodes[J]. *Science Advances*, 2024, 10(33): eado0614.

Author Biographies：

SANG Xi-en (1999—), Male, Zhumadian, Henan Province, Ph.D. enrolled in Zhengzhou University University for Ph.D. in 2024, mainly engaged in the research of nitride semiconductor devices and materials. E-mail: zzuxien@163.com

LIU Yu-huai (1969—), Male, Fuyang, Anhui, Ph.D., Professor, Ph.D. Supervisor, joined Zhengzhou University in 2011, worked in Japan from nitride semiconductor materials and devices research and product development for more than ten years. His research interests include the core technology of nitride semiconductor-based blue LEDs and LDs, UV LEDs, IR LDs and HBTs, HEMTs and other devices. E-mail: ieyhliu@zzu.edu.cn